

Activation of the sweet taste receptor, T1R3, by the artificial sweetener sucralose regulates the pulmonary endothelium

Elizabeth O Harrington^{1,2}, Alexander Vang¹, Julie Braza^{1,2}, Aparna Shil³, Havovi Chichger³

¹*Vascular Research Laboratory, Providence Veterans Affairs Medical Center,
Providence, RI 02908 USA*

²*Department of Medicine, Alpert Medical School of Brown University, Providence,
Rhode Island 02912 USA*

³*Biomedical Research Group, Anglia Ruskin University, Cambridge CB1 1PT UK*

Address correspondence to:

Havovi Chichger, Ph.D.
Biomedical Research Group
Department of Biomedical and Forensic Sciences
East Road
Cambridge, CB1 1PT, UK
E-mail: Havovi.Chichger@anglia.ac.uk

Running title: Sweet taste in the pulmonary endothelium

Keywords: pulmonary endothelium, sweet taste, acute respiratory distress syndrome, T1R3, artificial sweeteners

Word count: 3687 excluding abstract, legends and references

Number of figures: 7

Number of tables: 1

ABSTRACT

A hallmark of acute respiratory distress syndrome (ARDS) is pulmonary vascular permeability. In these settings, loss of barrier integrity is mediated by cell-contact disassembly and actin-remodelling. Studies into molecular mechanisms responsible for improving microvascular barrier function are therefore vital in the development of therapeutic targets for reducing vascular permeability in ARDS. The sweet taste receptor, T1R3 is a GPCR, activated following exposure to sweet molecules, to trigger a gustducin-dependent signal cascade. In recent years, extraoral locations for T1R3 have been identified however, no studies have focused on T1R3 within the vasculature. We hypothesise that activation of T1R3, in the pulmonary vasculature, plays a role in regulating endothelial barrier function in settings of ARDS.

Our study demonstrated expression of T1R3 within the pulmonary vasculature, with a drop in expression levels following exposure to barrier disruptive agents. Exposure of lung microvascular endothelial cells to the intensely sweet molecule, sucralose, attenuated LPS- and thrombin-induced endothelial barrier dysfunction. Likewise, sucralose exposure attenuated bacteria-induced lung edema formation *in vivo*. Inhibition of sweet taste signalling, through zinc sulfate, T1R3 or G-protein siRNA, blunted the protective effects of sucralose on the endothelium. Sucralose significantly reduced LPS-induced increased expression or phosphorylation of key signalling molecules, Src, PAK, MLC2, HSP27 and p110 α PI3K.

Activation of T1R3, by sucralose, protects the pulmonary endothelium from edemagenic agent-induced barrier disruption, potentially through abrogation of Src/PAK/p110 α PI3K-mediated cell-contact disassembly and Src/MLC2/HSP27-mediated actin-remodelling. Identification of sweet taste sensing in the pulmonary vasculature may represent a novel therapeutic target to protect the endothelium in settings of ARDS.

INTRODUCTION

Acute respiratory distress syndrome (ARDS) is a major cause of morbidity and mortality in patients suffering from several predisposing factors such as trauma, sepsis and pneumonia. The syndrome occurs when vascular fluid and protein leak across the pulmonary microvascular endothelium into the alveolar air space, causing pulmonary edema formation which is characteristic of the disease. Respiratory failure then occurs as a result of decreased gas exchange and lung compliance, and initiation of inflammatory cascades (79). Thus a key hallmark of ARDS is permeability of the pulmonary microvascular endothelium to vascular fluid and protein.

Vascular permeability is regulated through several mechanisms depending on the stimulus however each mechanism results in breakdown of cell-cell contacts and actin remodelling. Permeability of the monolayer occurs through disruption of cell-cell contacts, maintained by the adherens junction complex, and an increase in actin-myosin contractility (39, 40, 77). In the case of lipopolysaccharide (LPS), an endotoxin from gram-negative bacteria, endothelial permeability is mediated through its binding to toll-like receptor 4. The resulting Src-dependent signalling cascade leads to phosphorylation of both VE-cadherin and myosin light chain-2 (MLC2) (65, 71). Furthermore, expression of the heat shock protein families, HSP27, HSP 70 and HSP 90, correlates with increased vascular permeability (5, 32, 36). Targeting of these molecular mechanisms has been shown to attenuate LPS-induced pulmonary edema formation *in vivo* (3, 15), indicating the potential role for these molecules in settings of ARDS.

Members of the bitter taste receptor family, and their signalling effectors, have been identified in pulmonary solitary chemosensory cells (SCCs) (24, 37, 62, 67, 76), ciliated epithelial cells (64), and smooth muscle cells lining the airways (20). In pulmonary smooth muscle, 21 of the 25 members of the bitter taste receptor family have been identified with bitter taste agonists leading to vasodilation and bronchodilation (10, 20). While studies have identified other members of the taste receptor family in solitary chemosensory cells (SCCs), no functional output has been previously described (74). In recent years, sweet taste receptors have also been identified in extraoral locations, such as pancreatic beta cells, adipocytes and cardiomyocytes (6), however they have not been previously identified in the vasculature. Sweet taste is mediated by the G-protein coupled receptor (GPCR), T1R3, which can form a homodimer or a heterodimer with T1R2 (56). Sweet taste receptors are activated

upon binding of intensely sweet molecules, such as artificial sweeteners, at low concentrations (<1 mM) or glucose at high concentrations (>300 mM) (44). The consumption of artificial sweeteners has increased in recent years, with the concentration in diet soda ranging from 150 to 500 μ M (25). In humans, while the majority of artificial sweeteners consumed are excreted in faeces, a significant proportion are absorbed by the small intestine, identified within the circulation (plasma) and excreted in the urine as a non-metabolized molecule (60, 72). Therefore it is likely that, following consumption of a diet high in artificial sweeteners, the vasculature is exposed to high levels of these intensely sweet molecules.

In the studies presented here, we demonstrate, for the first time, the presence of the sweet taste receptor T1R3 in the pulmonary endothelium. Expression of the receptor was demonstrated to be modulated by barrier-disruptive agents however stimulation of T1R3, with the intensely sweet artificial molecule sucralose, attenuates thrombin- and LPS-induced endothelial monolayer permeability. Furthermore, *in vivo* exposure to sucralose attenuates lung edema formation induced by *Pseudomonas aeruginosa*. Our studies show that sucralose-mediated protection of the endothelial barrier is dependent on components of the sweet taste sensing pathway. Interestingly, exposure to high glucose does not protect the pulmonary endothelium. Finally, we implicate a role for HSP27, p110 α PI3K, MLC2, Src and PAK in sucralose-mediated protection of the pulmonary endothelium. Our studies demonstrate that sweet taste sensing at the pulmonary endothelium plays a key role in barrier function. Stimulation of the sweet taste receptor may represent a novel target in the treatment of ARDS.

METHODS

Cell lines and reagents

TRIzol and Superscript II (Invitrogen). Rat lung microvascular endothelial cells (LMVEC; Vec Technologies, Rensselaer, NY) were cultured in MCDB-131 media (Vec Technologies) and used between *passages 3* and *9*. LPS (endotoxin) from *Escherichia coli* serotype 011:B4, recombinant VEGF protein and thrombin were purchased from Sigma-Aldrich (St. Louis, MO, USA). *Pseudomonas aeruginosa* strain 103 (PA103) was a kind gift from Dr. Troy Stevens (University of South Alabama, Mobile, AL, USA). Gustducin (*GNAT3*) and gustducin siRNA were purchased from Origene (Rockville, MD, USA). T1R3 (*Tas1R3*) and Gαq siRNA were purchased from Santa Cruz Biotechnology (Santa Cruz, CA, USA).

In vivo studies

LPS or vehicle (saline) was administered to non-anesthetized, adult male 8- to 10-wk-old C57BL/6 mice via a single injection at different doses (1, 2.5 and 5 mg/kg i.p.). At 24 h following intraperitoneal injection of LPS or vehicle into mice, lungs were removed for homogenization. Untreated male Sprague-Dawley rats were euthanized at 8 weeks and both lungs and jejunal segments was isolated and stored in RNAlater (Thermo Scientific, Waltham, MA, USA) at –80 °C.

Mice were exposed to sucralose (1 g/kg) by oral gavage once a day for 1 week. At endpoint, live gram-negative bacteria *P. aeruginosa* (PA103) or PBS vehicle was administered via a single intratracheal injection [10^6 colony-forming units (CFUs)]. At 4 h following PA103 administration, wet and dry lung weights were taken.

All animal experimental protocols were approved by the Institutional Animal Care and Use Committees of the Providence Veterans Affairs Medical Center and Brown University and comply with the Health Research Extension Act and U.S. Public Health Service policy.

RT-PCR

Total RNAs were extracted from rat lung, jejunum and cultured LMVECs using the TRIzol reagent (Thermo Scientific, Waltham, MA, USA) as per the manufacturer's instructions. RNA was purified using the acid phenol/chloroform system and reverse transcribed using SuperScriptII (Thermo Scientific, Waltham, MA, USA) and T1R3 transcripts were measured

with β -actin (GenBank accession number NM_031144; forward 937-955, reverse 1223-1208) used as the house-keeping gene as described previously (8). Expression of the *Tas1r3* gene was measured using specific intron-spanning primers which were designed from the sequences published for rat (GenBank accession number NM_130818.1; forward 2107-2126, reverse 2327-2308). Relative gene expression level was analysed, for each sample, using the Δ Ct method where Δ Ct = (Ct_{Tas1r3} – Ct _{β -actin}) corresponding to the detected threshold cycles for the target gene and β -actin control.

Western blotting

LMVEC were exposed to LPS (1 μ g/ml) or sucralose (0.1 mM) for 24 hours. Cells were then lysed with RIPA buffer, resuspended in Laemmli buffer and subjected to immunoblot analysis. Individual lobes of mouse lungs were homogenized in buffer [20 mM 4-(2-hydroxyethyl)-1-piperazineethanesulfonic acid (HEPES) (pH7.9), 1.5 mM NaCl, 0.25 M sucrose, 0.2 mM EDTA, 200 mM PMSF, 0.5 mM DTT, and 1.5 mM MgCl₂] for 2 min and subjected to immunoblot analysis. Immunoblot analyses were performed on 10% SDS-PAGEs using a range of primary antibodies (table 1) at a dilution of 1:1000, except vinculin (1:5000), and secondary antibody dilutions of 1:5000. All samples were run on the same immunoblot for each protein analysed. Antibody specificity verification was assessed based on previous publications (included in table 1) or with siRNA knockout studies (Figure 5).

Endothelial monolayer permeability

Changes in endothelial monolayer permeability were assessed using the electrical cell impedance sensor (ECIS) technique (Applied Biophysics, Troy, NY), as previously described (16, 29). For analysis of monolayer permeability LMVEC were seeded to confluence onto collagen-coated electric cell-substrate impedance sensing arrays. For knockdown experiments, LMVECs were transiently transfected with T1R3, Gαq or gustducin siRNA duplexes (300 nM), or ns, scrambled control, using the Amaxa (Allendale, NJ, USA) electroporation technique as described previously (15). Monolayers were treated with either sucralose (0.1 mM), glucose (5.5 mM, 11 and 25 mM) or vehicle (H₂O) in the presence and absence of VEGF (50 ng/ml), thrombin (2 U/ml), LPS (1 μ g/ml) or zinc sulfate (0.7 mM). Addition of treatments were made at the same time and resistance was measured over time.

176 ***Statistical analysis***

177 For three or more groups, differences among the means were tested for significance
178 in all experiments by ANOVA with Fisher's least significance difference test. Significance was
179 reached when $p < 0.05$. Values are mean \pm standard deviation (SD).

180

181

182

RESULTS

Sweet taste receptor, T1R3, is expressed at the pulmonary endothelium

Sweet taste receptor T1R3 is the key component of the sweet taste complex – T1R3 is necessary for the heterodimeric complex but can also form a homodimer for sweet taste sensing (19, 50, 56). In addition to the oral cavity, high expression of T1R3 mRNA (*TAS1R3*) and protein has been found in the small intestine, in particular the jejunum (41). mRNA expression levels of *TAS1R3* in rat lungs and LMVEC were comparable to the positive control rat tissue (jejunum) (Figure 1a). To assess the link between sweet taste receptor and ARDS, protein expression of T1R3 was studied in LMVEC following exposure (24 h) to the barrier disruptive agents LPS, VEGF and thrombin, and in mouse lungs following exposure to LPS (4 h). In LMVEC, T1R3 protein levels were significantly reduced, to a similar degree, in the presence of all three agonists (Figure 1b). Expression of T1R3 in mouse lungs was unaffected at low concentrations of LPS (1 and 2.5 mg/kg) however at 5 mg/kg, where lung injury and vascular leak are observed (13, 15), T1R3 expression was significantly reduced (Figure 1c). This data demonstrates the presence of T1R3 in the lung microvasculature, and implicates sweet taste sensing in endothelial barrier function.

Artificial sweetener sucralose attenuates barrier disruption in vitro and in vivo

The sweet taste receptor complex is activated by low concentrations of intensely sweet molecules or high concentrations of sugars (51). Our previous studies demonstrate that endothelial permeability is closely related to adherens junction formation, with increased VE-cadherin surface levels observed in barrier protective settings (15). Therefore we next assessed whether activation of T1R3 with the artificial sweetener sucralose, at concentration close to EC_{50} (51), has an effect on endothelial barrier function and VE-cadherin surface expression. LMVEC exposed to sucralose displayed no change in endothelial monolayer resistance (Figure 2a, 2b, 3a and 3b) or VE-cadherin surface expression (Figure 2c and 3c). Interestingly, thrombin-induced permeability and loss of VE-cadherin surface expression was significantly attenuated by concomitant exposure of LMVEC to sucralose (Figure 2). Likewise, sucralose attenuated LPS-induced permeability and decrease in VE-cadherin surface levels (Figure 3). We next sought to establish whether sucralose exerted a protective effect on *in vivo* lung edema formation (wet-to-dry lung weight). Mice were exposed to a daily oral dose of sucralose over a 1 week period, followed by exposure to *P. aeruginosa* (PA103) as a model

for acute lung injury. Similar to *in vitro* findings, sucralose exposure significantly attenuated PA103-induced lung edema formation *in vivo* (Figure 3d). Interestingly, sucralose exposure in the absence of PA103 had no effect on lung edema formation. Interestingly, both LPS- and thrombin-induced permeability *in vitro* and PA103-induced edema formation *in vivo* was not completely reversed by sucralose however the artificial sweetener did result in surface expression levels of VE-cadherin returning to baseline levels (Figure 2 and 3).

We next assessed whether glucose regulates endothelial barrier function in a similar manner. LMVEC were exposed to increasing concentrations of glucose from fasting levels (5.5 mM) to hyperglycaemic levels (25 mM), with an osmotic control of mannose used for the high glucose concentration, in the presence and absence of LPS. High glucose (25 mM), but not lower glucose concentrations or mannose, significantly increased endothelial permeability and decreased VE-cadherin surface levels under baseline conditions (Figure 4a and b). LPS-induced permeability and decreased VE-cadherin surface levels was significantly exacerbated in the presence of high glucose, but not lower glucose concentrations or mannose (Figure 4a and b). Interestingly, exposure of LMVEC to sucralose significantly increased protein levels of T1R3, whilst high glucose had no effect on expression of the sweet taste receptor (Figure 4c).

Taken together, these data indicate that the intensely sweet molecule sucralose, but not high physiological levels of glucose, regulates T1R3 to protect the pulmonary endothelium against barrier disruption.

Barrier-protective effect of sucralose is mediated through sensing by the sweet taste receptor

To study whether sucralose acts on the endothelial monolayer in a T1R3-dependent manner, the next experiments utilised inhibitors of the sweet taste receptor pathway. Molecular and chemical inhibition of T1R3 was performed using siRNA knockdown (Figure 5a) and exposure to zinc sulfate (Figure 5b) a chemical inhibitor of sweet taste receptor (23, 38). Endothelial permeability was assessed in the presence and absence of LPS and sucralose. Interestingly, attenuation of LPS-induced permeability by sucralose was significantly blocked by molecular (Figure 5a) and chemical (Figure 5b) inhibition of T1R3. In the presence of LPS alone, T1R3 inhibition had no impact on endothelial permeability (Figure 5a and b). Molecular inhibition of gustducin, a key signalling molecule downstream of T1R3 (53), was performed

using siRNA knockdown (Figure 5ci). Knockdown of gustducin, had no effect on endothelial permeability in settings of either LPS or sucralose exposure (Figure 5cii). Molecular inhibition of gustducin significantly abrogated sucralose-mediated protection of LPS-induced permeability (Figure 5cii). The G protein, Gαq, which is highly expressed in the lung has also been identified to play a role in sweet taste sensing (75, 80). Molecular inhibition of Gαq was performed in LMVEC using siRNA (Figure 5di). Protection of LPS-induced permeability, by sucralose, was reduced by 21% following knockdown of Gαq (Figure 5d). These data indicate that sucralose exerts a protective effect on the endothelium, in settings of barrier disruption, through regulation of the sweet taste receptor and the downstream signalling pathway.

Sucralose attenuates LPS-induced elevated HSP27 and p110α and activation of MLC2, Src and PAK

To assess the molecular mechanism through which sucralose exerts an effect on LPS-induced signalling, key regulators of the adherens junction and endothelial barrier function were assessed for expression and activity. Phosphorylation of kinases FAK, p38, ERK, PAK, p70 and Src (15, 28), phosphatase SHP2 (14), filament proteins VASP and cofilin (59, 67), and MLC2 (7) were measured at phosphorylation sites relevant to protein activity (Table 1). Expression of heat shock proteins HSP27, 70 and 90 (11, 36, 45) and the p110αPI3K (9) were also assessed. Sucralose treatment, in the absence of LPS, had no effect on phosphorylation or expression of any regulator molecule (Figure 6 and 7). Phosphorylation of MLC2, Src and PAK by LPS was significantly attenuated by exposure to sucralose (Figure 6 a, 6b and 6c), whereas phosphorylation of other key regulators was unaffected by sucralose (Figure 7a-g). Unlike MLC2 and Src, in the presence of sucralose and LPS, phosphorylation of PAK did not return to baseline conditions (Figure 6a, 6b and 6c). Expression levels of HSP27 and p110αPI3K were increased following exposure to LPS however this effect was abrogated by sucralose (Figure 6d and 6e). This effect was not observed in the other heat shock proteins, HSP70 and 90 (Figure 7h and 7i). Taken together, these data indicate that sucralose may attenuate LPS-induced permeability through inhibition of key barrier disruptive signaling molecules.

DISCUSSION

In the present study we demonstrate, for the first time, the localisation and function of the sweet taste receptor at the pulmonary endothelium. Our research identified the expression of T1R3 in the lung and microvascular endothelial cells, with reduced protein levels in response to the barrier-disruptive agents LPS, thrombin and VEGF. We observed that activation of T1R3, by exposure to the artificial sweetener sucralose, protects the microvasculature *in vitro* and *in vivo* against barrier disruptive agents, through a sweet taste receptor-dependent pathway. Lastly, we implicated a role for sucralose in attenuating LPS-mediated Src, PAK, MLC2, HSP27 and p110 α PI3K signalling. Therefore the stimulation of T1R3, by artificial sweetener sucralose, represents a novel mechanism through which the pulmonary microvasculature is regulated.

The sweet taste receptor, T1R3, was first identified at the *Sac* genetic locus, which regulates sweet taste sensitivity, with expression observed in a subset of taste cells within the oral cavity (52, 54). Interestingly, T1R3 has recently been identified in extraoral locale, including the pancreatic beta cell, adipocytes and the bladder, however to date, no studies have assessed T1R3 in the vasculature (23, 55, 66, 73). Our study identifies T1R3 mRNA expression in the rat lung and microvascular endothelial cells. Interestingly, mRNA levels of both were similar to those observed in the jejunum segment of the small intestine. Studies by others and us have identified T1R3 in different cell types within the small intestine, predominantly the jejunum, where activation of the receptor is linked to altered glucose metabolism in patients with metabolic diseases (8, 47, 49, 69). Therefore T1R3 expression in the pulmonary vasculature is likely to be at a physiologically significant level. Endothelial cell protein expression of T1R3 was reduced by the barrier disruptive agents LPS, thrombin and VEGF. This was mirrored in the mouse lung where decreased T1R3 levels were noted following LPS treatment. Interestingly, at low doses of LPS, where no pulmonary edema is observed (data not shown), T1R3 expression is not significantly affected however at 5 mg/kg dose, where pulmonary edema is observed (13, 15), T1R3 expression was significantly reduced. Therefore it is likely that T1R3 expression plays a role in pulmonary endothelial barrier maintenance *in vivo* and *in vitro*. Indeed, following exposure to sucralose, which activates T1R3, barrier permeability caused by LPS and thrombin was attenuated. These findings were mirrored in an *in vivo* model of lung injury (*P. aeruginosa*), with sucralose exposure blocking lung edema formation. The *in vitro* protective role of sucralose was blocked

following inhibition of sweet taste sensing, either by acting on the receptor via zinc sulfate (23, 38) or siRNA knockdown of T1R3 or downstream G proteins gustducin and Gαq (53, 75). Inhibition of T1R3, through siRNA or zinc sulfate, attenuated the protective effect of sucralose on the endothelial barrier. The artificial sweetener is therefore acting through the sweet taste receptor to initiate a protective signalling response. Interestingly, Gαq inhibition did not completely blunt sucralose-mediated protection as seen in gustducin inhibition. It is therefore likely that gustducin, but not Gαq, is essential for T1R3-mediated signalling in the pulmonary endothelium.

Signalling mechanisms mediated by activated T1R3 vary depending on the cell type. In the pancreatic beta cell, sweetener-T1R3 binding results in insulin release mediated by elevated intracellular calcium levels (55) whilst in the adipocyte, Akt phosphorylation was noted to play a role in the stimulation of adipogenesis (66). In the pulmonary endothelium, studies presented here link the phosphorylation of Src, PAK and MLC2, and increased expression of HSP27 and p110αPI3K, with sucralose-mediated protection from LPS. Previous studies have indicated a key role for Src and PAK phosphorylation, and p110αPI3K expression, in the breakdown of the pulmonary endothelium through dissolution of the adherens junction (9, 12, 15, 28) and in HSP27 and MLC2-mediated actin remodelling associated with barrier disruption (27, 32, 65, 71). Interestingly, other key regulators of the pulmonary endothelium, such as the filament proteins cofilin and VASP (59, 67) are phosphorylated by LPS but unaffected by sucralose. Thus, upon activation, T1R3 acts on a limited range of signalling molecules to regulate endothelial barrier function. The link between signalling downstream of T1R3 and Src/PAK/p110αPI3K and HSP27/MLC2 is unclear at present however it is possible that PLCβ2 recruitment, following release of gustducin and Gαq, triggers the activation of kinases such as the inhibitory Src kinase Csk (48, 81). This in turn may regulate downstream molecules to protect the endothelial barrier from LPS-induced disruption. However further studies are necessary to identify and understand the molecular mechanisms through which T1R3 downstream signalling regulates Src/PAK/p110αPI3K and HSP27/MLC2 within the pulmonary endothelium.

Sucralose is an intensely sweet, commercially-available artificial sweetener with an estimated 'sweetness' index of 600-times compared to sucrose (57). Sucralose, like many artificial sweeteners, stimulates the sweet taste receptor at low concentrations (<1 mM) (44). At glucose concentrations needed to stimulate T1R3 (>300 mM), endothelial cells are not

342 viable due to hyperosmolarity (1, 21). We demonstrate that, at a physiologically relevant high
343 concentration of glucose (25 mM), vascular permeability was increased. Similar to previous
344 studies, we also observed that high glucose exacerbates LPS-mediated barrier disruption (46)
345 therefore the protective effect of T1R3 activation, with sucralose, cannot be mimicked by
346 glucose. Furthermore, whilst this study focused on the use of sucralose to activate T1R3,
347 different artificial sweeteners demonstrate varying ability to bind T1R3 and stimulate
348 downstream signalling (56). It is therefore possible that the level of pulmonary barrier
349 protection exhibited by the sweetener is dependent on the type of sweet molecule used.

350 There is significant controversy regarding the benefit of artificial sweetener
351 consumption in the diet. At present, a large proportion of the population consumes artificial
352 sweeteners, such as sucralose, at high levels (25) however clinical studies do not record any
353 pulmonary responses in this population. Interestingly, our studies show that exposure of the
354 microvasculature to sucralose, in the absence of LPS, has no effect on barrier function or on
355 the expression or activation of key signalling molecules which regulate the endothelium.
356 Therefore it is possible that stimulation of T1R3, by artificial sweeteners, only plays a
357 physiological role in settings of vascular permeability. This represents the potential for
358 artificial sweeteners to act as a novel therapeutic agent in diseases such as ARDS, however
359 further studies are necessary to assess the long-term effect of artificial sweeteners on the
360 pulmonary vasculature. Whilst the present study only assessed T1R3 expression, as it is the
361 predominant sweet taste receptor which homodimerises to sense sweet molecules, T1R2 can
362 form a heterodimer with T1R3 and form a sweet taste receptor complex (56). Furthermore,
363 T1R3 can heterodimerise with T1R1 to form an umami taste receptor complex. As our study
364 demonstrates a significant protective effect played by the sweet taste receptor in the
365 pulmonary endothelium, it would be interesting to assess other taste sensing complexes
366 within the vasculature. In fact, previous studies have implicated that stimulation of the bitter
367 taste receptor family (T2R) in airway smooth muscle and epithelial cells, with bitter taste
368 agonists, stimulates bronchodilation and ciliary beat frequency respectively (20, 64). Bitter
369 agonists are currently under scrutiny as a treatment for asthma and COPD patients (42, 61,
370 68) however studies are yet to assess the presence or activation of bitter taste receptors
371 within the pulmonary vasculature. Our studies demonstrate that sweet taste agonists block
372 the barrier disruptive effects of LPS on the pulmonary endothelium. There is therefore the
373 potential for taste agonists to play a major role in various lung diseases in the future.

374

375

376

377

378

ACKNOWLEDGEMENTS

This material is based on work supported by Diabetes UK Grant 15/0005284, Wellcome Trust Grant UNS22596 and American Heart Association Grant 13POST16860031 (H. Chichger). E. O. Harrington was supported by the National Heart, Lung, and Blood Institute Grant R01 HL-67795 and R01 HL-123965 and by an Institutional Development Award (IDeA) from the National Institute of General Medical Sciences of the National Institutes of Health under grant number P20 GM103652. A. Vang was supported by National Heart, Lung, and Blood Institute Grant 1R01HL128661. The views expressed in this article are those of the authors and do not necessarily reflect the position or policy of the Department of Veterans Affairs.

AUTHOR CONTRIBUTIONS

Acquisition of data: HC, AV, JB, AS
Conception and design: HC, EOH
Analysis and interpretation: HC, AS, AV
Drafting the manuscript for intellectual content: HC, EOH

CONFLICT OF INTEREST DISCLOSURE

The authors have nothing to disclose.

398 REFERENCES

- 399 1. **Abe M, Ono J, Sato Y, Okeda T and Takaki R.** Effects of glucose and insulin on cultured
400 human microvascular endothelial cells. *Diabetes Res.Clin.Pract.* 9: 3: 287-295, 1990.
- 401 2. **Alvarado AG, Thiagarajan PS, Mulkearns-Hubert EE, Silver DJ, Hale JS, Alban TJ, Turaga**
402 **SM, Jarrar A, Reizes O, Longworth MS, Vogelbaum MA and Lathia JD.** Glioblastoma Cancer
403 Stem Cells Evade Innate Immune Suppression of Self-Renewal through Reduced TLR4
404 Expression. *Cell.Stem Cell.* 20: 4: 450-461.e4, 2017.
- 405 3. **Antonov A, Snead C, Gorshkov B, Antonova GN, Verin AD and Catravas JD.** Heat shock
406 protein 90 inhibitors protect and restore pulmonary endothelial barrier function.
407 *Am.J.Respir.Cell Mol.Biol.* 39: 5: 551-559, 2008.
- 408 4. **Aoki T, Tsunekawa K, Araki O, Ogiwara T, Nara M, Sumino H, Kimura T and Murakami M.**
409 Type 2 Iodothyronine Deiodinase Activity Is Required for Rapid Stimulation of PI3K by
410 Thyroxine in Human Umbilical Vein Endothelial Cells. *Endocrinology* 156: 11: 4312-4324,
411 2015.
- 412 5. **Barabutis N, Handa V, Dimitropoulou C, Rafikov R, Snead C, Kumar S, Joshi A, Thangjam**
413 **G, Fulton D, Black SM, Patel V and Catravas JD.** LPS induces pp60c-src-mediated tyrosine
414 phosphorylation of Hsp90 in lung vascular endothelial cells and mouse lung.
415 *Am.J.Physiol.Lung Cell.Mol.Physiol.* 304: 12: L883-93, 2013.
- 416 6. **Behrens M and Meyerhof W.** Gustatory and extragustatory functions of mammalian taste
417 receptors. *Physiol.Behav.* 105: 1: 4-13, 2011.
- 418 7. **Birukova AA, Adyshev D, Gorshkov B, Bokoch GM, Birukov KG and Verin AD.** GEF-H1 is
419 involved in agonist-induced human pulmonary endothelial barrier dysfunction.
420 *Am.J.Physiol.Lung Cell.Mol.Physiol.* 290: 3: L540-8, 2006.
- 421 8. **Bueter M, Miras AD, Chichger H, Fenske W, Ghattei MA, Bloom SR, Unwin RJ, Lutz TA,**
422 **Spector AC and le Roux CW.** Alterations of sucrose preference after Roux-en-Y gastric bypass.
423 *Physiol.Behav.* 104: 5: 709-721, 2011.
- 424 9. **Cain RJ, Vanhaesebroeck B and Ridley AJ.** The PI3K p110alpha isoform regulates
425 endothelial adherens junctions via Pyk2 and Rac1. *J.Cell Biol.* 188: 6: 863-876, 2010.
- 426 10. **Chandrashekar J, Mueller KL, Hoon MA, Adler E, Feng L, Guo W, Zuker CS and Ryba NJ.**
427 T2Rs function as bitter taste receptors. *Cell* 100: 6: 703-711, 2000.

428 11. **Chatterjee A, Snead C, Yetik-Anacak G, Antonova G, Zeng J and Catravas JD.** Heat shock
429 protein 90 inhibitors attenuate LPS-induced endothelial hyperpermeability.
430 *Am.J.Physiol.Lung Cell.Mol.Physiol.* 294: 4: L755-63, 2008.

431 12. **Check J, Byrd CL, Menio J, Rippe RA, Hines IN and Wheeler MD.** Src kinase participates in
432 LPS-induced activation of NADPH oxidase. *Mol.Immunol.* 47: 4: 756-762, 2010.

433 13. **Chichger H, Braza J, Duong H, Boni G and Harrington EO.** Select Rab GTPases Regulate
434 the Pulmonary Endothelium via Endosomal Trafficking of Vascular Endothelial-Cadherin.
435 *Am.J.Respir.Cell Mol.Biol.* 54: 6: 769-781, 2016.

436 14. **Chichger H, Braza J, Duong H and Harrington EO.** SH2 domain-containing protein tyrosine
437 phosphatase 2 and focal adhesion kinase protein interactions regulate pulmonary
438 endothelium barrier function. *Am.J.Respir.Cell Mol.Biol.* 52: 6: 695-707, 2015.

439 15. **Chichger H, Duong H, Braza J and Harrington EO.** p18, a novel adaptor protein, regulates
440 pulmonary endothelial barrier function via enhanced endocytic recycling of VE-cadherin.
441 *FASEB J.* 29: 3: 868-881, 2015.

442 16. **Chichger H, Grinnell KL, Casserly B, Chung CS, Braza J, Lomas-Neira J, Ayala A, Rounds S,**
443 **Klinger JR and Harrington EO.** Genetic disruption of protein kinase Cdelta reduces endotoxin-
444 induced lung injury. *Am.J.Physiol.Lung Cell.Mol.Physiol.* 303: 10: L880-8, 2012.

445 17. **Chichger H, Vang A, O'Connell KA, Zhang P, Mende U, Harrington EO and Choudhary G.**
446 PKC delta and betaII regulate angiotensin II-mediated fibrosis through p38: a mechanism of
447 RV fibrosis in pulmonary hypertension. *Am.J.Physiol.Lung Cell.Mol.Physiol.* 308: 8: L827-36,
448 2015.

449 18. **Couch BA, Kerrisk ME, Kaufman AC, Nygaard HB, Strittmatter SM and Koleske AJ.**
450 Delayed amyloid plaque deposition and behavioral deficits in outcrossed AbetaPP/PS1 mice.
451 *J.Comp.Neurol.* 521: 6: 1395-1408, 2013.

452 19. **Damak S, Rong M, Yasumatsu K, Kokrashvili Z, Varadarajan V, Zou S, Jiang P, Ninomiya**
453 **Y and Margolske RF.** Detection of sweet and umami taste in the absence of taste receptor
454 T1r3. *Science* 301: 5634: 850-853, 2003.

455 20. **Deshpande DA, Wang WC, McIlmoyle EL, Robinett KS, Schillinger RM, An SS, Sham JS**
456 **and Liggett SB.** Bitter taste receptors on airway smooth muscle bronchodilate by localized
457 calcium signaling and reverse obstruction. *Nat.Med.* 16: 11: 1299-1304, 2010.

458 21. **Duffy A, Liew A, O'Sullivan J, Avalos G, Samali A and O'Brien T.** Distinct effects of high-
459 glucose conditions on endothelial cells of macrovascular and microvascular origins.
460 *Endothelium* 13: 1: 9-16, 2006.

461 22. **Durkin CH, Leite F, Cordeiro JV, Handa Y, Arakawa Y, Valderrama F and Way M.** RhoD
462 Inhibits RhoC-ROCK-Dependent Cell Contraction via PAK6. *Dev.Cell.* 41: 3: 315-329.e7, 2017.

463 23. **Elliott RA, Kapoor S and Tincello DG.** Expression and distribution of the sweet taste
464 receptor isoforms T1R2 and T1R3 in human and rat bladders. *J.Urol.* 186: 6: 2455-2462, 2011.

465 24. **Finger TE, Bottger B, Hansen A, Anderson KT, Alimohammadi H and Silver WL.** Solitary
466 chemoreceptor cells in the nasal cavity serve as sentinels of respiration.
467 *Proc.Natl.Acad.Sci.U.S.A.* 100: 15: 8981-8986, 2003.

468 25. **Franz M.** Diet soft drinks: how safe are they? *Diabetes Self Manag.* 27: 2: 8, 11-13, 2010.

469 26. **Gallo D, Gesmundo I, Trovato L, Pera G, Gargantini E, Minetto MA, Ghigo E and Granata**
470 **R.** GH-Releasing Hormone Promotes Survival and Prevents TNF-alpha-Induced Apoptosis and
471 Atrophy in C2C12 Myotubes. *Endocrinology* 156: 9: 3239-3252, 2015.

472 27. **Garcia JG, Davis HW and Patterson CE.** Regulation of endothelial cell gap formation and
473 barrier dysfunction: role of myosin light chain phosphorylation. *J.Cell.Physiol.* 163: 3: 510-522,
474 1995.

475 28. **Gavard J and Gutkind JS.** VEGF controls endothelial-cell permeability by promoting the
476 beta-arrestin-dependent endocytosis of VE-cadherin. *Nat.Cell Biol.* 8: 11: 1223-1234, 2006.

477 29. **Grinnell KL, Chichger H, Braza J, Duong H and Harrington EO.** Protection against LPS-
478 induced pulmonary edema through the attenuation of protein tyrosine phosphatase-1B
479 oxidation. *Am.J.Respir.Cell Mol.Biol.* 46: 5: 623-632, 2012.

480 30. **Havekes R, Park AJ, Tudor JC, Luczak VG, Hansen RT, Ferri SL, Bruinenberg VM, Poplawski**
481 **SG, Day JP, Aton SJ, Radwanska K, Meerlo P, Houslay MD, Baillie GS and Abel T.** Sleep
482 deprivation causes memory deficits by negatively impacting neuronal connectivity in
483 hippocampal area CA1. *Elife* 5: 10.7554/eLife.13424, 2016.

484 31. **Hill SM, Nesser NK, Johnson-Camacho K, Jeffress M, Johnson A, Boniface C, Spencer SE,**
485 **Lu Y, Heiser LM, Lawrence Y, Pande NT, Korkola JE, Gray JW, Mills GB, Mukherjee S and**
486 **Spellman PT.** Context Specificity in Causal Signaling Networks Revealed by Phosphoprotein
487 Profiling. *Cell.Syst.* 4: 1: 73-83.e10, 2017.

488 32. **Hirano S, Rees RS, Yancy SL, Welsh MJ, Remick DG, Yamada T, Hata J and Gilmont RR.**
489 Endothelial barrier dysfunction caused by LPS correlates with phosphorylation of HSP27 in
490 vivo. *Cell Biol.Toxicol.* 20: 1: 1-14, 2004.

491 33. **Hu JK, Du W, Shelton SJ, Oldham MC, DiPersio CM and Klein OD.** An FAK-YAP-mTOR
492 Signaling Axis Regulates Stem Cell-Based Tissue Renewal in Mice. *Cell.Stem Cell.* 21: 1: 91-
493 106.e6, 2017.

494 34. **Jeannot P, Nowosad A, Perchey RT, Callot C, Bennana E, Katsube T, Mayeux P,**
495 **Guillonneau F, Manenti S and Besson A.** p27Kip1 promotes invadopodia turnover and
496 invasion through the regulation of the PAK1/Cortactin pathway. *Elife* 6: 10.7554/eLife.22207,
497 2017.

498 35. **Jiang X, Chen J, Zhang C, Zhang Z, Tan Y, Feng W, Skibba M, Xin Y and Cai L.** The protective
499 effect of FGF21 on diabetes-induced male germ cell apoptosis is associated with up-regulated
500 testicular AKT and AMPK/Sirt1/PGC-1alpha signaling. *Endocrinology* 156: 3: 1156-1170, 2015.

501 36. **Kang Q, Chen Y, Zhang X, Yu G, Wan X, Wang J, Bo L and Zhu K.** Heat shock protein A12B
502 protects against sepsis-induced impairment in vascular endothelial permeability. *J.Surg.Res.*
503 202: 1: 87-94, 2016.

504 37. **Kaske S, Krasteva G, Konig P, Kummer W, Hofmann T, Gudermann T and Chubanov V.**
505 TRPM5, a taste-signaling transient receptor potential ion-channel, is a ubiquitous signaling
506 component in chemosensory cells. *BMC Neurosci.* 8: 49, 2007.

507 38. **Keast RS, Canty TM and Breslin PA.** Oral zinc sulfate solutions inhibit sweet taste
508 perception. *Chem.Senses* 29: 6: 513-521, 2004.

509 39. **Komarova Y and Malik AB.** Regulation of endothelial permeability via paracellular and
510 transcellular transport pathways. *Annu.Rev.Physiol.* 72: 463-493, 2010.

511 40. **Kuppers V, Vockel M, Nottebaum AF and Vestweber D.** Phosphatases and kinases as
512 regulators of the endothelial barrier function. *Cell Tissue Res.* 355: 3: 577-586, 2014.

513 41. **Le Gall M, Tobin V, Stolarczyk E, Dalet V, Leturque A and Brot-Laroche E.** Sugar sensing
514 by enterocytes combines polarity, membrane bound detectors and sugar metabolism.
515 *J.Cell.Physiol.* 213: 3: 834-843, 2007.

516 42. **Levit A, Nowak S, Peters M, Wiener A, Meyerhof W, Behrens M and Niv MY.** The bitter
517 pill: clinical drugs that activate the human bitter taste receptor TAS2R14. *FASEB J.* 28: 3: 1181-
518 1197, 2014.

519 43. **Li P, Liu S, Lu M, Bandyopadhyay G, Oh D, Imamura T, Johnson AM, Sears D, Shen Z, Cui**
520 **B, Kong L, Hou S, Liang X, Iovino S, Watkins SM, Ying W, Osborn O, Wollam J, Brenner M and**
521 **Olefsky JM.** Hematopoietic-Derived Galectin-3 Causes Cellular and Systemic Insulin
522 Resistance. *Cell* 167: 4: 973-984.e12, 2016.

523 44. **Li X, Staszewski L, Xu H, Durick K, Zoller M and Adler E.** Human receptors for sweet and
524 umami taste. *Proc.Natl.Acad.Sci.U.S.A.* 99: 7: 4692-4696, 2002.

525 45. **Liu T, Guevara OE, Warburton RR, Hill NS, Gaestel M and Kayyali US.** Modulation of
526 HSP27 alters hypoxia-induced endothelial permeability and related signaling pathways.
527 *J.Cell.Physiol.* 220: 3: 600-610, 2009.

528 46. **Liu XJ, Zhang ZD and Ma XC.** High glucose enhances LPS-stimulated human PMVEC
529 hyperpermeability via the NO pathway. *Exp.Ther.Med.* 6: 2: 361-367, 2013.

530 47. **Mace OJ, Affleck J, Patel N and Kellett GL.** Sweet taste receptors in rat small intestine
531 stimulate glucose absorption through apical GLUT2. *J.Physiol.* 582: Pt 1: 379-392, 2007.

532 48. **Margolskee RF.** Molecular mechanisms of bitter and sweet taste transduction.
533 *J.Biol.Chem.* 277: 1: 1-4, 2002.

534 49. **Margolskee RF, Dyer J, Kokrashvili Z, Salmon KS, Ilegems E, Daly K, Maillet EL, Ninomiya**
535 **Y, Mosinger B and Shirazi-Beechey SP.** T1R3 and gustducin in gut sense sugars to regulate
536 expression of Na⁺-glucose cotransporter 1. *Proc.Natl.Acad.Sci.U.S.A.* 104: 38: 15075-15080,
537 2007.

538 50. **Masubuchi Y, Nakagawa Y, Ma J, Sasaki T, Kitamura T, Yamamoto Y, Kurose H, Kojima I**
539 **and Shibata H.** A novel regulatory function of sweet taste-sensing receptor in adipogenic
540 differentiation of 3T3-L1 cells. *PLoS One* 8: 1: e54500, 2013.

541 51. **Masuda K, Koizumi A, Nakajima K, Tanaka T, Abe K, Misaka T and Ishiguro M.**
542 Characterization of the modes of binding between human sweet taste receptor and low-
543 molecular-weight sweet compounds. *PLoS One* 7: 4: e35380, 2012.

544 52. **Max M, Shanker YG, Huang L, Rong M, Liu Z, Campagne F, Weinstein H, Damak S and**
545 **Margolskee RF.** Tas1r3, encoding a new candidate taste receptor, is allelic to the sweet
546 responsiveness locus Sac. *Nat.Genet.* 28: 1: 58-63, 2001.

547 53. **McLaughlin SK, McKinnon PJ and Margolskee RF.** Gustducin is a taste-cell-specific G
548 protein closely related to the transducins. *Nature* 357: 6379: 563-569, 1992.

549 54. **Montmayeur JP, Liberles SD, Matsunami H and Buck LB.** A candidate taste receptor gene
550 near a sweet taste locus. *Nat.Neurosci.* 4: 5: 492-498, 2001.

551 55. **Nakagawa Y, Nagasawa M, Yamada S, Hara A, Mogami H, Nikolaev VO, Lohse MJ,**
552 **Shigemura N, Ninomiya Y and Kojima I.** Sweet taste receptor expressed in pancreatic beta-
553 cells activates the calcium and cyclic AMP signaling systems and stimulates insulin secretion.
554 *PLoS One* 4: 4: e5106, 2009.

555 56. **Nelson G, Hoon MA, Chandrashekar J, Zhang Y, Ryba NJ and Zuker CS.** Mammalian sweet
556 taste receptors. *Cell* 106: 3: 381-390, 2001.

557 57. **Olivier B, Serge AH, Catherine A, Jacques B, Murielle B, Marie-Chantal CL, Sybil C, Jean-**
558 **Philippe G, Sabine H, Esther K, Perrine N, Fabienne R, Gerard S and Irene M.** Review of the
559 nutritional benefits and risks related to intense sweeteners. *Arch.Public.Health.* 73: 41-015-
560 0092-x. eCollection 2015, 2015.

561 58. **Prunier C, Josserand V, Vollaire J, Beerling E, Petropoulos C, Destaing O, Montemagno**
562 **C, Hurbin A, Prudent R, de Koning L, Kapur R, Cohen PA, Albiges-Rizo C, Coll JL, van Rheenen**
563 **J, Billaud M and Lafanechere L.** LIM Kinase Inhibitor Pyr1 Reduces the Growth and Metastatic
564 Load of Breast Cancers. *Cancer Res.* 76: 12: 3541-3552, 2016.

565 59. **Rentsendorj O, Mirzapoiazova T, Adyshev D, Servinsky LE, Renne T, Verin AD and Pearce**
566 **DB.** Role of vasodilator-stimulated phosphoprotein in cGMP-mediated protection of human
567 pulmonary artery endothelial barrier function. *Am.J.Physiol.Lung Cell.Mol.Physiol.* 294: 4:
568 L686-97, 2008.

569 60. **Roberts A, Renwick AG, Sims J and Snodin DJ.** Sucralose metabolism and
570 pharmacokinetics in man. *Food Chem.Toxicol.* 38 Suppl 2: S31-41, 2000.

571 61. **Robinett KS, Koziol-White CJ, Akoluk A, An SS, Panettieri RA,Jr and Liggett SB.** Bitter taste
572 receptor function in asthmatic and nonasthmatic human airway smooth muscle cells.
573 *Am.J.Respir.Cell Mol.Biol.* 50: 4: 678-683, 2014.

574 62. **Sbarbati A, Merigo F, Benati D, Tizzano M, Bernardi P, Crescimanno C and Osculati F.**
575 Identification and characterization of a specific sensory epithelium in the rat larynx.
576 *J.Comp.Neurol.* 475: 2: 188-201, 2004.

577 63. **Sclip A, Bacaj T, Giam LR and Sudhof TC.** Extended Synaptotagmin (ESyt) Triple Knock-Out
578 Mice Are Viable and Fertile without Obvious Endoplasmic Reticulum Dysfunction. *PLoS One*
579 11: 6: e0158295, 2016.

580 64. **Shah AS, Ben-Shahar Y, Moninger TO, Kline JN and Welsh MJ.** Motile cilia of human
581 airway epithelia are chemosensory. *Science* 325: 5944: 1131-1134, 2009.

582 65. **Shen Q, Rigor RR, Pivetti CD, Wu MH and Yuan SY.** Myosin light chain kinase in
583 microvascular endothelial barrier function. *Cardiovasc.Res.* 87: 2: 272-280, 2010.

584 66. **Simon BR, Parlee SD, Learman BS, Mori H, Scheller EL, Cawthorn WP, Ning X, Gallagher**
585 **K, Tyrberg B, Assadi-Porter FM, Evans CR and MacDougald OA.** Artificial sweeteners
586 stimulate adipogenesis and suppress lipolysis independently of sweet taste receptors.
587 *J.Biol.Chem.* 288: 45: 32475-32489, 2013.

588 67. **Slee JB and Lowe-Krentz LJ.** Actin realignment and cofilin regulation are essential for
589 barrier integrity during shear stress. *J.Cell.Biochem.* 114: 4: 782-795, 2013.

590 68. **Spina D.** Current and novel bronchodilators in respiratory disease. *Curr.Opin.Pulm.Med.*
591 20: 1: 73-86, 2014.

592 69. **Steinert RE, Gerspach AC, Gutmann H, Asarian L, Drewe J and Beglinger C.** The functional
593 involvement of gut-expressed sweet taste receptors in glucose-stimulated secretion of
594 glucagon-like peptide-1 (GLP-1) and peptide YY (PYY). *Clin.Nutr.* 30: 4: 524-532, 2011.

595 70. **Straussman R, Morikawa T, Shee K, Barzily-Rokni M, Qian ZR, Du J, Davis A, Mongare**
596 **MM, Gould J, Frederick DT, Cooper ZA, Chapman PB, Solit DB, Ribas A, Lo RS, Flaherty KT,**
597 **Ogino S, Wargo JA and Golub TR.** Tumour micro-environment elicits innate resistance to RAF
598 inhibitors through HGF secretion. *Nature* 487: 7408: 500-504, 2012.

599 71. **Sun H, Breslin JW, Zhu J, Yuan SY and Wu MH.** Rho and ROCK signaling in VEGF-induced
600 microvascular endothelial hyperpermeability. *Microcirculation* 13: 3: 237-247, 2006.

601 72. **Sweatman TW, Renwick AG and Burgess CD.** The pharmacokinetics of saccharin in man.
602 *Xenobiotica* 11: 8: 531-540, 1981.

603 73. **Taniguchi K.** Expression of the sweet receptor protein, T1R3, in the human liver and
604 pancreas. *J.Vet.Med.Sci.* 66: 11: 1311-1314, 2004.

605 74. **Tizzano M, Cristofolletti M, Sbarbati A and Finger TE.** Expression of taste receptors in
606 solitary chemosensory cells of rodent airways. *BMC Pulm.Med.* 11: 3-2466-11-3, 2011.

607 75. **Tizzano M, Dvoryanchikov G, Barrows JK, Kim S, Chaudhari N and Finger TE.** Expression
608 of Galpha14 in sweet-transducing taste cells of the posterior tongue. *BMC Neurosci.* 9: 110-
609 2202-9-110, 2008.

610 76. **Tizzano M, Gulbransen BD, Vandenbeuch A, Clapp TR, Herman JP, Sibhatu HM, Churchill**
611 **ME, Silver WL, Kinnamon SC and Finger TE.** Nasal chemosensory cells use bitter taste
612 signaling to detect irritants and bacterial signals. *Proc.Natl.Acad.Sci.U.S.A.* 107: 7: 3210-3215,
613 2010.

614 77. **Trani M and Dejana E.** New insights in the control of vascular permeability: vascular
615 endothelial-cadherin and other players. *Curr.Opin.Hematol.* 22: 3: 267-272, 2015.

616 78. **Tsai MJ, Yang-Yen HF, Chiang MK, Wang MJ, Wu SS and Chen SH.** TCTP is essential for
617 beta-cell proliferation and mass expansion during development and beta-cell adaptation in
618 response to insulin resistance. *Endocrinology* 155: 2: 392-404, 2014.

- 619 79. **Welbourn CR and Young Y.** Endotoxin, septic shock and acute lung injury: neutrophils,
620 macrophages and inflammatory mediators. *Br.J.Surg.* 79: 10: 998-1003, 1992.
- 621 80. **Wilkie TM, Scherle PA, Strathmann MP, Slepak VZ and Simon MI.** Characterization of G-
622 protein alpha subunits in the Gq class: expression in murine tissues and in stromal and
623 hematopoietic cell lines. *Proc.Natl.Acad.Sci.U.S.A.* 88: 22: 10049-10053, 1991.
- 624 81. **Zhang SQ, Yang W, Kontaridis MI, Bivona TG, Wen G, Araki T, Luo J, Thompson JA,**
625 **Schraven BL, Philips MR and Neel BG.** Shp2 regulates SRC family kinase activity and Ras/Erk
626 activation by controlling Csk recruitment. *Mol.Cell* 13: 3: 341-355, 2004.
- 627 82. **Zhang X, Spiegelman NA, Nelson OD, Jing H and Lin H.** SIRT6 regulates Ras-related protein
628 R-Ras2 by lysine defatty-acylation. *Elife* 6: 10.7554/eLife.25158, 2017.
- 629

FIGURE LEGENDS

Figure 1: Expression of the sweet taste receptor, T1R3, at the pulmonary endothelium is regulated by barrier disruptive agents. *Panel a:* mRNA expression of the T1R3 gene, *Tas1r3*, in rat lung and jejunum tissue and cultured rat LMVEC. Gene expression is relative to the housekeeping gene, β -actin, and normalized to the positive control jejunum tissue. $n = 6$. *Panel b and c:* Protein expression of T1R3 in: (b) cultured rat LMVEC exposed to LPS (1 μ g/ml), thrombin (2 U/ml) or VEGF (50 ng/ml) for 24 hours and (c) homogenates of lungs from C57/BL6 mice exposed to varying doses of LPS (0 - 5 mg/kg). $n = 5$. A representative blot (i) and densitometry relative to the load control, β -actin (ii) are shown. Data is expressed as mean \pm S.D. * $p < 0.05$ versus vehicle.

Figure 2: Stimulation of the artificial sweetener sucralose attenuates thrombin-induced barrier disruption and VE-cadherin internalisation. *Panels a and b:* Changes in rat LMVEC endothelial monolayer resistance were measured using ECIS in the presence (closed symbols) and absence (open symbols) of thrombin (2 U/ml). Monolayers were exposed to sucralose (0.1 mM) (triangle symbols), or vehicle (H_2O) (square symbols) at the same time as thrombin. Permeability is shown as (a) an experimental trace, normalised to the addition of thrombin and sucralose (arrow), and (b) drop in endothelial resistance measured at 12 minutes post-thrombin and sucralose treatment. $n = 5$. *Panel c:* Cell surface expression of VE-cadherin was determined, with whole-cell indirect ELISA using chemiluminescence, following exposure to thrombin and sucralose as per (a). $n = 6$. Data is expressed as mean \pm S.D. * $p < 0.05$ versus vehicle for thrombin, # $p < 0.05$ vs vehicle for sucralose.

Figure 3: Stimulation of the artificial sweetener sucralose attenuates LPS-induced barrier disruption and VE-cadherin internalisation *in vitro* and bacteria-induced edema formation *in vivo*. *Panels a and b:* Changes in rat LMVEC endothelial monolayer resistance were measured using ECIS in the presence (closed symbols) and absence (open symbols) of LPS (1 μ g/ml). Monolayers were exposed to sucralose (0.1 mM) (triangle symbols), or vehicle (H_2O) (square symbols) at the same time as LPS. Permeability is shown as (a) an experimental trace, normalised to the addition of LPS and sucralose (arrow), and (b) drop in endothelial resistance measured at 10 hours. $n = 5$. *Panel c:* Cell surface expression of VE-cadherin was determined,

with whole-cell indirect ELISA using chemiluminescence, following exposure to LPS and sucralose as per (a). *n* = 6. *Panel d*: Lung edema formation was determined by measuring wet-to-dry lung weight ratio in mice following daily gavage of sucralose (1 g/kg) for 1 week and 4 hour exposure to *P. aeruginosa* (PA103). *n*=5-8. Data is expressed as mean \pm S.D. **p*<0.05 versus vehicle for LPS, #*p*<0.05 vs vehicle for sucralose.

Figure 4: High glucose exposure increases endothelial barrier permeability and VE-cadherin internalisation. *Panel a*: Changes in rat LMVEC endothelial monolayer resistance (*panel a*) were measured using ECIS in the presence (closed bars) and absence (open bars) of LPS (1 μ g/ml). Monolayers were exposed to different concentrations of glucose (5.5, 11 and 25 mM) or osmotic control mannose (25 mM) at the same time as LPS. Permeability is shown as drop in endothelial resistance measured at 10 hours. *n* = 5. *Panel b*: Cell surface expression of VE-cadherin was determined, with whole-cell indirect ELISA using chemiluminescence, following exposure to LPS and glucose as per (a). *Panel c*: Protein expression of T1R3 in cultured rat LMVEC exposed to sucralose (0.1 mM), glucose (25 mM) or vehicle for both (H₂O) for 24 hours. A representative blot (*upper panel*) and densitometry relative to the load control, β -actin (*lower panel*) are shown. *n* = 5. Data is expressed as mean \pm S.D. **p*<0.05 versus vehicle for LPS, #*p*<0.05 versus 5.5 mM control.

Figure 5: Barrier-protective effect of sucralose is mediated through sensing by the sweet taste receptor. *Panels a, c and d*: Equivalent numbers of rat LMVECs were transiently transfected with scrambled (300 nM, open bars) or T1R3 (300 nM, closed bars) siRNA (*panel a ii*), gustducin (Gus, 300 nM, closed bars) siRNA (*panel c ii*) or Gαq (300 nM, closed bars) siRNA (*panel d ii*). Following 48 hours, changes in endothelial monolayer resistance were measured using ECIS in the presence and absence of LPS (1 μ g/ml) and sucralose (0.1 mM). Permeability is shown as drop in endothelial resistance measured at 10 hours (*ii*). Knockdown of endogenous protein was confirmed by immunoblot analysis of lysates from transiently transfected cells with an antibody specific to T1R3 (*panel a i*), gustducin (*panel c i*) and Gαq (*panel d i*). *Panel b*: Monolayer permeability was assessed in the presence and absence of the sweet taste inhibitor zinc sulfate (0.7 mM). Changes in endothelial monolayer resistance were measured using ECIS in the presence and absence of LPS (1 μ g/ml) and sucralose (0.1 mM). Permeability is shown as drop in endothelial resistance measured at 10 hours. *n* = 5-6.

Data is expressed as mean \pm S.D. * $p < 0.05$ versus vehicle for LPS, [^] $p < 0.05$ vs vehicle for sucralose, [#] $p < 0.05$ versus LPS + vehicle for sucralose.

Figure 6: Sucralose attenuates LPS-induced elevated HSP27 and p110 α PI3K and activation of MLC2, Src and PAK. Rat LMVECs were treated in the presence or absence of LPS (1 μ g/ml) and sucralose (0.1 mM) for 24 hours. Phosphorylation of MLC-2 (a), Src (b) and PAK (c) was assessed in whole-cell lysates by immunoblot analysis with an antibody specific to each phosphorylated protein. Blots were stripped and reprobed for total protein expression and actin as a loading control. Total protein expression of HSP27 (d) and p110 α PI3K (e) was also assessed in whole-cell lysates, followed strip and reprobe of blots for actin as a loading control. Representative blots are shown. Non-essential lanes from the HSP27 representative blot (panel d) have been removed. $n = 6$. Data is expressed as mean \pm S.D. * $p < 0.05$ versus vehicle for LPS, [#] $p < 0.05$ vs vehicle for sucralose.

Figure 7: Role of sucralose on LPS-mediated signalling is independent of several key molecules. Rat LMVECs were treated in the presence or absence of LPS (1 μ g/ml) and sucralose (0.1 mM) for 24 hours. Phosphorylation of HSP70 (a), SHP2 (b), ERK (c), FAK (d), VASP (e), p38 (f) and cofilin (g) was assessed in whole-cell lysates by immunoblot analysis with an antibody specific to each phosphorylated protein. Blots were stripped and reprobed for total protein expression and actin as a loading control. Total protein expression of HSP70 (h) and HSP90 (i) was also assessed in whole-cell lysates, followed strip and reprobe of blots for actin as a loading control. Representative blots are shown. $n = 6$. Data is expressed as mean \pm S.D. * $p < 0.05$ versus vehicle for LPS.

TABLE

Table 1: List of antibodies used for protein phosphorylation (panel a) and expression (panel b) analysis by Western blot.

a

Antibody	Company	Phospho site
Phospho-Cofilin	Cell Signaling (30)	Serine 3
Phospho-MLC2	Cell Signaling (22)	Threonine 18 / serine 19
Phospho-VASP	Cell Signaling (31)	Serine 239
Phospho-PAK 1/2	Cell Signaling (33)	Threonine 423/402
Phospho-Src	Cell Signaling (4)	Tyrosine 416
Phospho-ERK1/2	Cell Signaling (70)	Threonine 202 / tyrosine 204
Phospho-p38	Cell Signaling (17)	Threonine 180 / tyrosine 182
Phospho-p70 (T389)	Cell Signaling (78)	Threonine 389
Phospho-FAK (Y397)	Cell Signaling (12)	Tyrosine 397
Phospho-SHP2 (Y542)	Santa Cruz (12)	Tyrosine 452

b

Antibody	Company
HSP90	BD Biosciences (43)
FAK	BD Bioscience (12)
HSP70	BD Biosciences (18)
Cofilin	Cell Signaling (58)
VASP	Cell Signaling (31)

PAK1	Cell Signaling (4) 727
MLC2	Cell Signaling (22)
ERK1/2	Cell Signaling (35)
p38	Cell Signaling (17)
Src	Santa Cruz (34)
SHP2	Santa Cruz (12)
p70	Santa Cruz (26)
T1R3	Santa Cruz
β -actin	Santa Cruz (2)
G α q	Santa Cruz
p110 α PI3K	Santa Cruz (82)
Gustducin	Santa Cruz
HSP27	Santa Cruz (63)

728

729

Figure 1

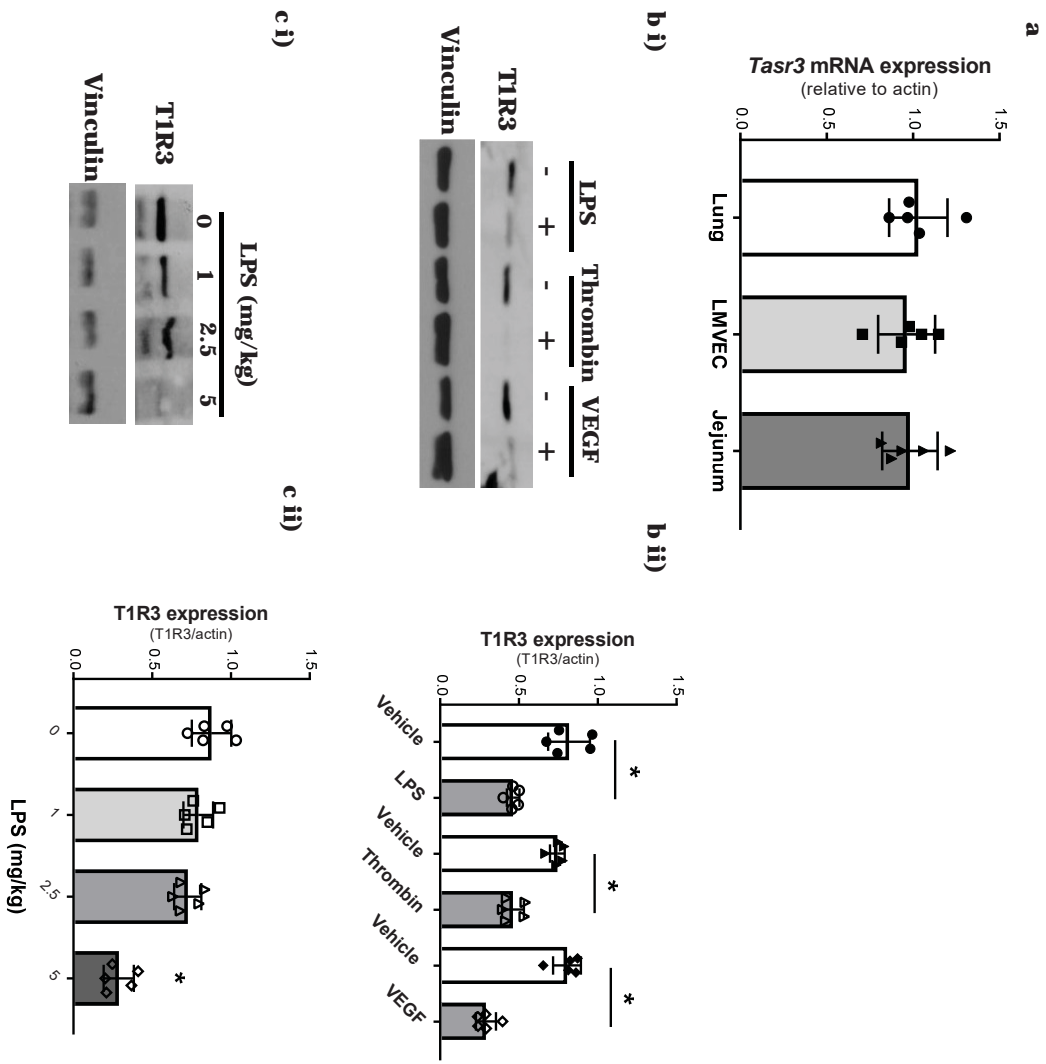


Figure 2

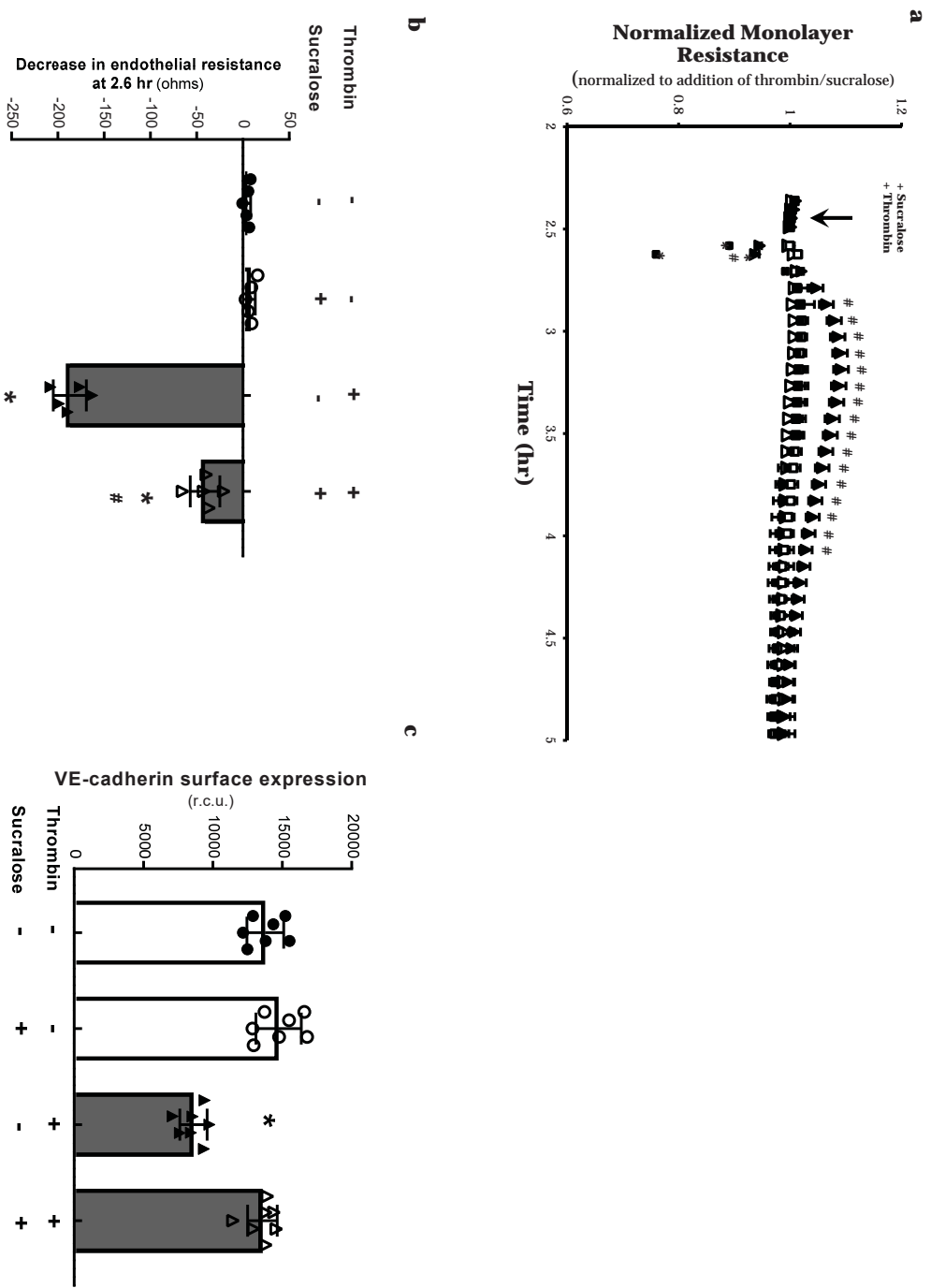


Figure 3

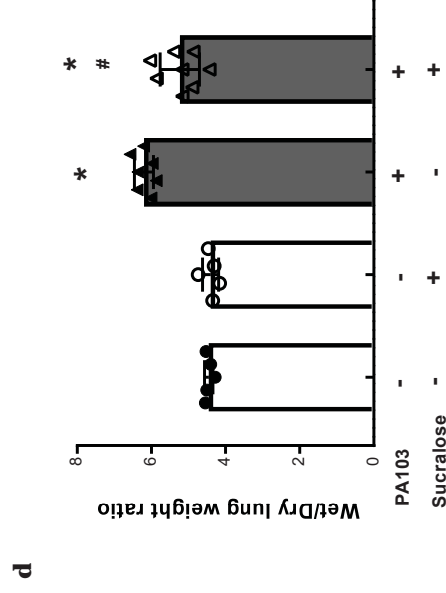
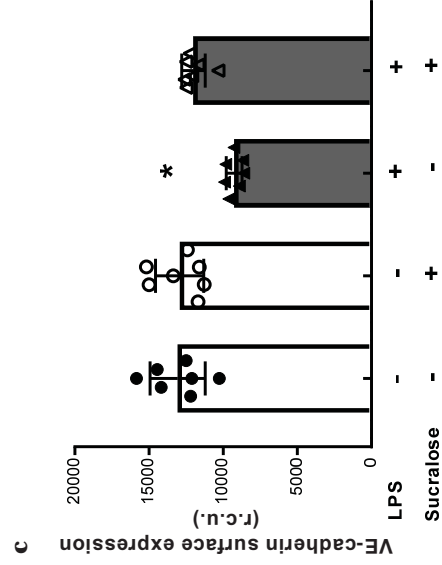
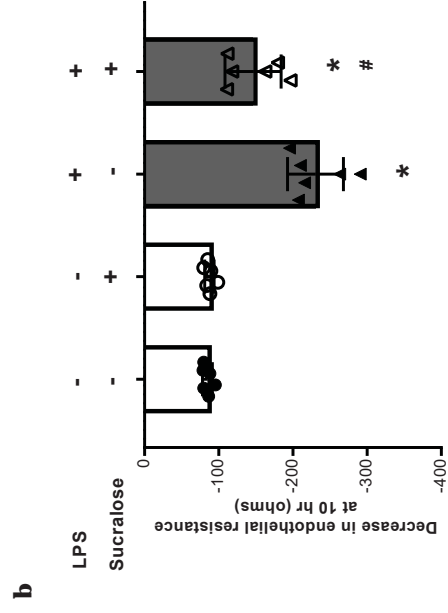
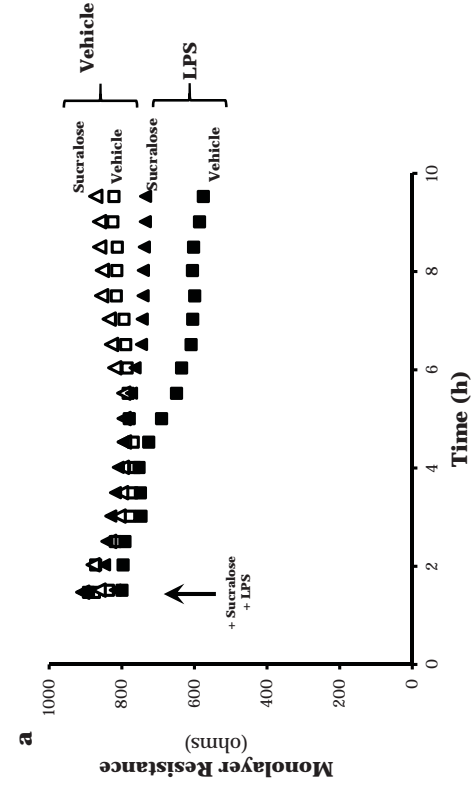


Figure 4

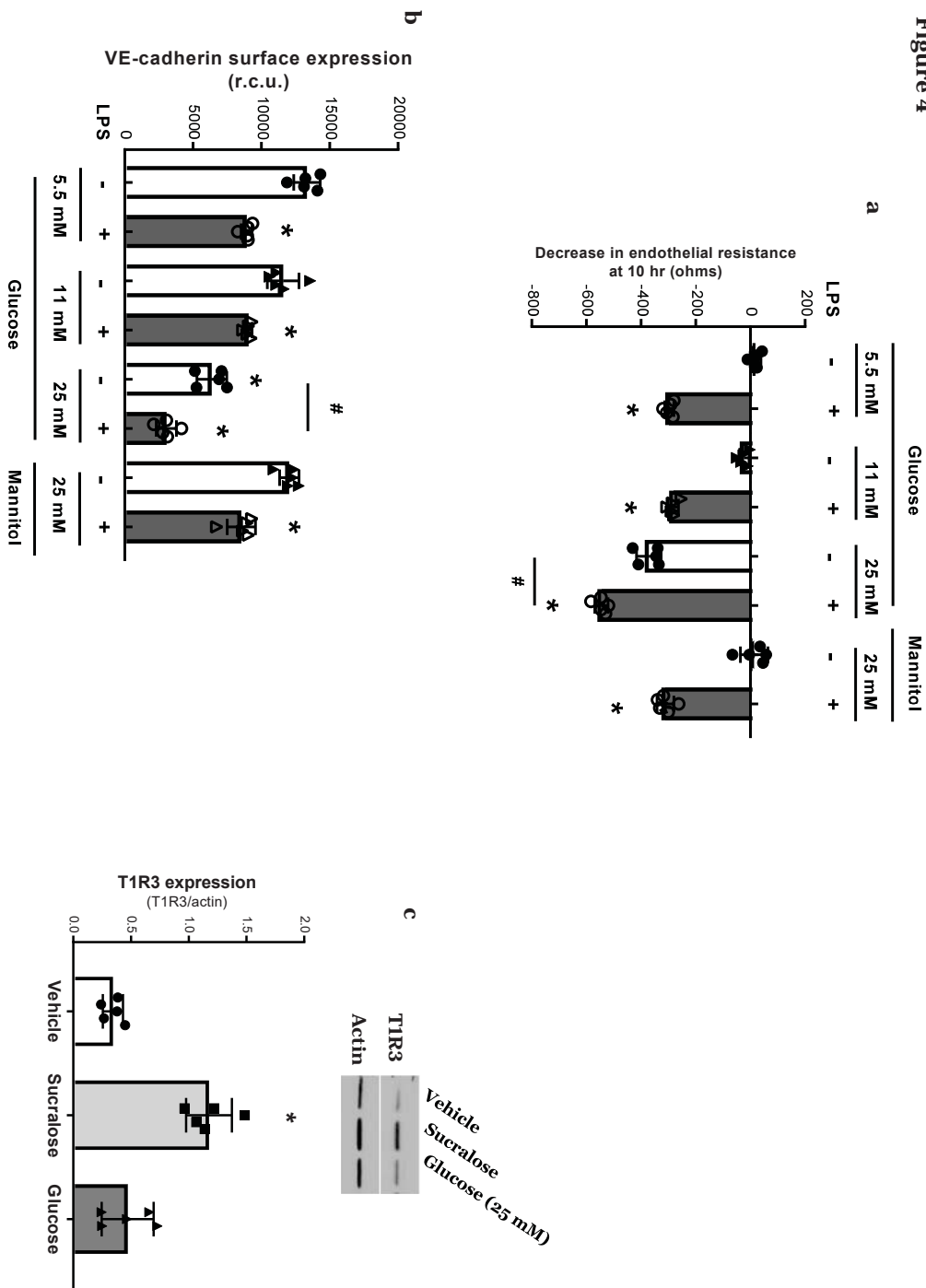


Figure 5

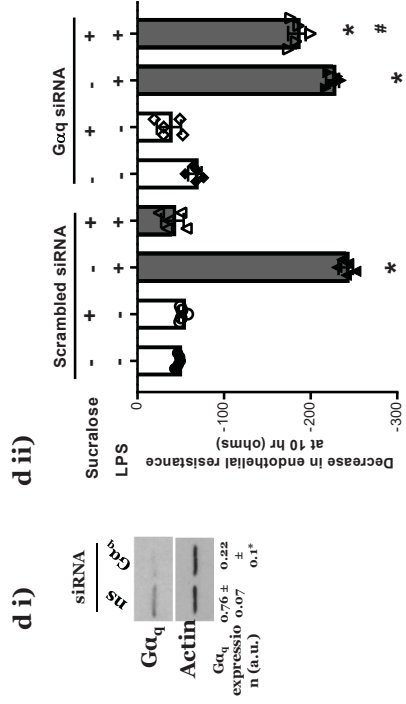
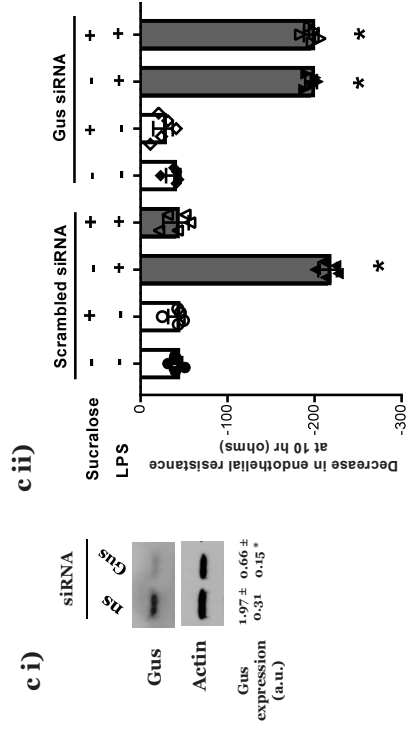
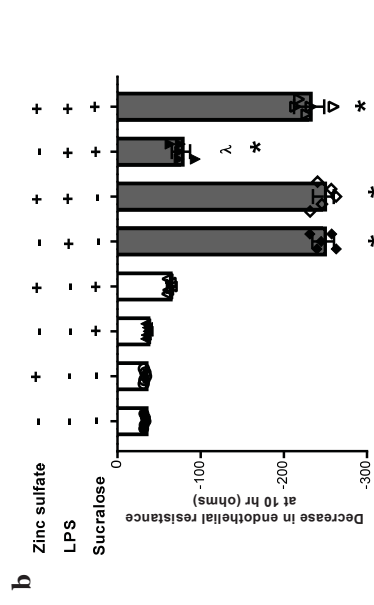
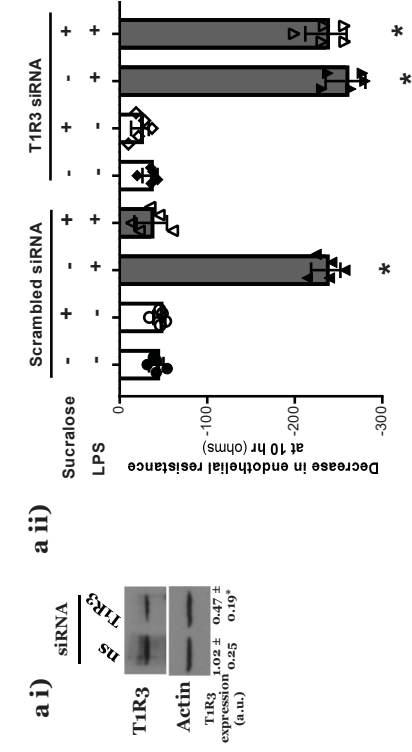


Figure 6

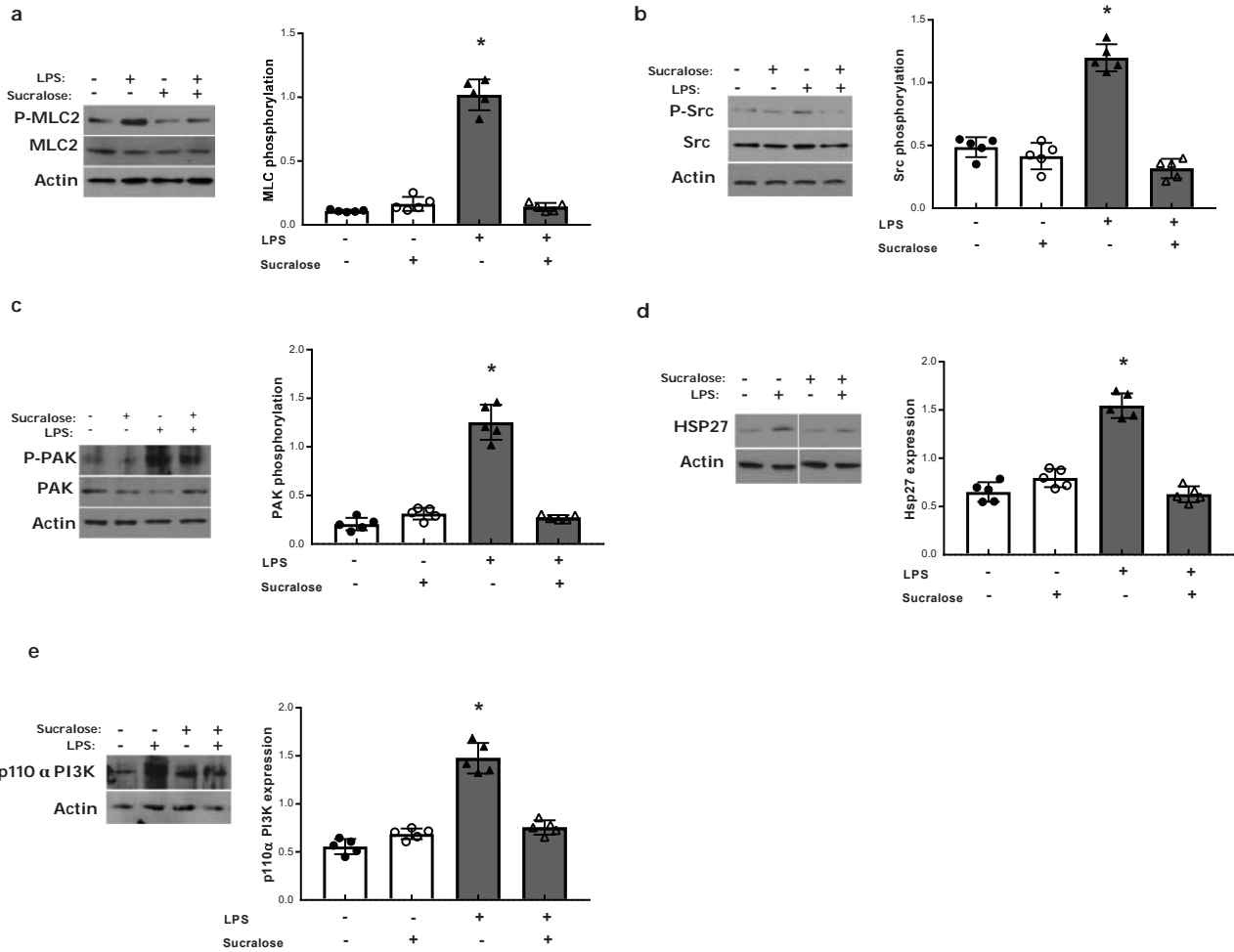


Figure 7

